AIP | The Journal of Chemical Physics

Numerical self-consistent field theory study of the response of strong polyelectrolyte brushes to external electric fields

Chaohui Tong

Citation: The Journal of Chemical Physics **143**, 054903 (2015); doi: 10.1063/1.4927814
View online: http://dx.doi.org/10.1063/1.4927814
View Table of Contents: http://scitation.aip.org/content/aip/journal/jcp/143/5?ver=pdfcov
Published by the AIP Publishing

Numerical self-consistent field theory study of the response of strong polyelectrolyte brushes to external electric fields

Chaohui Tong[a)]
Department of Physics, Ningbo University, Ningbo, Zhejiang 315211, China

(Received 4 February 2015; accepted 23 July 2015; published online 5 August 2015)

The response of strong polyelectrolyte (PE) brushes grafted on an electrode to electric fields generated by opposite surface charges on the PE-grafted electrode and a second parallel electrode has been numerically investigated by self-consistent field theory. The influences of grafting density, average charge fraction, salt concentration, and mobile ion size on the variation of the brush height against an applied voltage bias were investigated. In agreement with molecular dynamics simulation results, a higher grafting density requires a larger magnitude of voltage bias to achieve the same amount of relative change in the brush height. In the experimentally relevant parameter regime of the applied voltage, the brush height becomes insensitive to the voltage bias when the grafting density is high. Including the contribution of surface charges on the grafting electrode, overall charge neutrality inside the PE brushes is generally maintained, especially for PE brushes with high grafting density and high average charge fraction. Our numerical study further reveals that the electric field across the two electrodes is highly non-uniform because of the complex interplay between the surface charges on the electrodes, the charges on the grafted PE chains, and counterions. [http://dx.doi.org/10.1063/1.4927814]

I. INTRODUCTION

Polyelectrolyte (PE) brushes are composed of polymer chains with ionizable functional groups densely grafted onto solid substrates by covalent bonds or physical adsorption.[1–4] When immersed in a polar solvent (e.g., water), the functional groups along the polymer chains dissociate and release counterions into the solution, resulting in charged polymer chains. PE brushes can be classified into two types according to the nature of the ionizable functional groups. The first type is strong PE brushes, in which the ionizable functional groups completely dissociate in water (ignoring charge condensation, i.e., Manning condensation). The second type is weak PE brushes, in which the ionizable functional groups participate in an acid–base ionization equilibrium. Grafting PE chains provides a useful way to modify and regulate material surface properties. PE brushes have been extensively used in many technological applications, such as surface modification, colloidal stabilization, lubrication, and smart materials. Thus, it is not surprising that PE brushes have been intensively investigated by theory[5–11] and simulations.[12–27]

A very important application of PE brushes is in sensing and actuation because of the conformational change of grafted polymer chains in response to external stimuli. Owing to the long-range nature of the Coulomb interaction, the conformational behavior of PE brushes is much richer than their neutral counterparts and sensitively depends on a number of factors, such as grafting density, average degree of ionization, pH, and salt concentration. Moreover, the presence of electric charges along PE chains and the associated counterions enables PE brushes to respond to an electric field applied normal to the grafting substrate. Compared with other stimuli, the electrical stimulus represents a more advantageous way to regulate the polymer chain conformations because it can be easily and instantaneously switched on or off, remotely controlled, and fully automated.[28–31] Zhou and co-workers reported electroactuation of microcantilevers with strong PE brushes grafted on one side.[32] Very strong cantilever deflection was observed by alternating the electric potential on the cantilever between 0.5 and −0.5 V at frequencies up to 0.25 Hz.[32] The mechanism of actuation is based on the reversible perturbation of the electric double layer and conformational changes of the grafted PE chains. They also developed a mean-field theory to correlate the conformational changes of the grafted polymer chains with the reorganization of ions because of the potential bias. Very recently, the pH-responsive behavior of weak PE brushes coupled to an external electrical stimulus generated by an electrolysis device, which can switch the brush height and create waves of swelling or collapse of PE brushes, has been reported.[33]

Because of their technological importance, the response of PE brushes to an applied electric field or voltage is attracting considerable theoretical and computational research interest. Using self-consistent field theory (SCFT) and strong-stretching theory, Migliorini investigated the stretching and contraction of PE and neutral polymer brushes with a charged terminal group under electric fields generated by the similarly or oppositely charged grafting surface.[34] Tsori and co-workers investigated the response of a polymer brush with a charged terminal group to external electric fields using a

a)Author to whom correspondence should be addressed. Electronic mail: tongchaohui@nbu.edu.cn. Tel.: 86+057487600919. Fax: 86+057487600744.

coarse-grained continuum theoretical model.[35] Yamamoto and Pincus theoretically investigated the collapse of a strong polyacid grafted on an electrode in an applied electric field in the limiting cases of low and high salt concentrations.[36] Using SCFT, Meng and Wang numerically investigated the extension and contraction of strong polyacid brushes under the influence of positive or negative surface charges on the grafting substrate.[37] Using molecular dynamics (MD) simulations, Ouyang and co-workers investigated the static and dynamic responses of strong polyacid PE brushes to an external electric field normal to the grafting substrate and opposite to the polymer chain extension direction.[28,31] Partial and full stretching of PE brushes under the electric field was observed. The stretching of strong polyacid PE chains grafted on an electrode and immersed in a salt-free solution subject to a normal and uniform electric field was recently investigated using MD simulations.[38] A key finding in this study was that the population of grafted polyelectrolyte chains split into two subpopulations. At a low grafting density around the crossover from the mushroom to brush regimes, most of the chains are stretched and only a minority remains unstretched. Conversely, at a grafting density corresponding to a true brush regime, most PE chains remain unstretched and only a small fraction are highly stretched.

In MD simulations of the response of strong PE brushes to external electric fields, a constant and spatially uniform electric field $\vec{E}$ is applied such that an electric force $\vec{F} = -\alpha_p |e| \vec{E}$ will act on each charged monomer with a charge fraction α_p. Such a model setup is, in terms of the external electric field, straightforward and convenient to implement in simulation. However, it precludes direct and quantitative comparison with experiments, in which an electric potential bias is applied to two parallel electrodes with one grafted with PE chains. However, the scope of previous numerical SCFT studies of strong PE brushes subject to external electric fields is quite limited and the model setup in these studies does not conform to a real experimental system, which includes two electrodes. Thus, a detailed and systematic investigation of the influences of system parameters, such as grafting density, charge fraction, and salt concentration, on the response of strong PE brushes to electric fields generated by two oppositely charged electrodes corresponding to the real experimental system is required.

In this paper, we present a systematic numerical SCFT study of the response of a strong PE brush grafted on an electrode to external electric fields that are generated by the opposite charges on the grafting electrode and a second parallel electrode. In this study, we pay particular attention to the influences of grafting density, charge fraction, and added monovalent salt ions on the variation of the brush height with the applied electric voltage. Furthermore, we investigate the effect of the size of mobile ions on the response of PE brushes to electric fields. The rest of the paper is organized as follows. In Section II, the theory and methods used in the present paper are described. In Section III, results and discussions concerning the influences of grafting density, average charge fraction, salt concentration, and the size of mobile ions on the dependence of the brush height on applied voltage are presented. In Section IV, the main results in this paper are summarized and conclusions are drawn.

II. THEORETICAL METHODS

In the system considered in this work, a strong PE brush (corresponding to a smeared charge distribution) was sandwiched between two parallel planar electrodes with separation D. A Cartesian coordinate system was constructed such that the x axis is normal to the electrodes. PE chains with a chain length of N were uniformly grafted onto one electrode at $x = 0$. The grafting density is denoted as σ_g (in units of number of chains per unit area). Monomers with a fixed charge fraction or average degree of ionization α_p carry negative charges and release positive monovalent counterions in aqueous solution. It was assumed that the two electrodes were connected to an external electric circuit driven by an electric power source, resulting in a surface charge density of σ_e (in units of number of elementary charges per unit area and $\sigma_e = 0, >0$, or <0) and $-\sigma_e$ on the electrodes at $x = 0$ and $x = D$, respectively. Furthermore, in this numerical study, the surface electric potential of the second electrode at $x = D$ was fixed at zero. Hence, the electric potential on the surface of the electrode grafted with PE chains is equivalent to the voltage applied across the two electrodes. To the aqueous solution confined between the two electrodes, monovalent salt (e.g., NaCl) was added with a resulting salt molar concentration of C_s.

SCFT for charged polymer systems treats the many-chain problem as an effective single flexible charged chain in a mean-field, which is determined self-consistently.[39,40] Compared with SCFT for neutral polymers, inside the Hamiltonian, the electrostatic contribution has the form $\int d\vec{r} \left[\psi(\vec{r})\hat{\rho}_e(\vec{r}) - \varepsilon\left|\vec{\nabla}\psi(\vec{r})\right|^2/2\right]$, where ε, ψ, and $\hat{\rho}_e$ are the dielectric permittivity of the medium, electric potential, and total charge density, respectively. Minimizing the free energy functional with respect to the field variables leads to a set of SCF equations. Within SCFT, the dimensionless mean-field SCF equations for the case of mobile point charges are

$$\phi_p(\vec{r}) + \phi_S(\vec{r}) - 1 = 0, \tag{1}$$

$$\omega_p(\vec{r}) = \chi_{PS} N \phi_S(\vec{r}) + \eta(\vec{r}), \tag{2}$$

$$\omega_S(\vec{r}) = \chi_{PS} N \phi_p(\vec{r}) + \eta(\vec{r}), \tag{3}$$

$$\omega_\pm(\vec{r}) = N\nu_\pm\psi(\vec{r}), \tag{4}$$

$$\phi_p(\vec{r}) = \frac{\bar{\phi}_p}{Q_p}\int_0^1 ds q_f(\vec{r},s)\, q_g(\vec{r},1-s), \tag{5}$$

$$\phi_M(\vec{r}) = \frac{\bar{\phi}_M}{Q_M}\exp\left[-\omega_M(\vec{r})/N\right], \tag{6}$$

$$\vec{\nabla}\cdot\left[\varepsilon(\vec{r})\vec{\nabla}\psi(\vec{r})\right] = -N\left[\alpha_p\nu_p\phi_p(\vec{r}) + \nu_+\phi_+(\vec{r}) + \nu_-\phi_-(\vec{r})\right], \tag{7}$$

where $\phi_j(\vec{r})$ with $j = P, S$, and $\pm$ are the dimensionless volume fractions of monomers, solvent molecules, and the number densities of mobile ions, respectively, $\eta(\vec{r})$ is the Lagrange multiplier to enforce the incompressibility condition, χ_{PS} is the Flory–Huggins interaction parameter between monomers and solvent molecules, and $\omega_j(\vec{r})$ is the conjugate potential field within the SCFT formalism. The volume-averaged densities $\bar{\phi}_p = n_p N/(\rho_0 V)$ and $\bar{\phi}_M \equiv n_M/(\rho_0 V)$, where n_p and n_M are the total number of grafted PE chains and species M ($M = S$, $+$, and $-$). $\varepsilon(\vec{r})$ is the dielectric permittivity. $Q_p = \int d\vec{r} q_f(\vec{r},s) q_g(\vec{r},1-s)/V$ (Q_p is independent of the

parameter s) and $Q_M = \int d\vec{r} \exp\left[-\omega_M/N\right]/V$, where V is the volume of the system. The monomers and the solvent molecules are assumed to be of equal size, i.e., $a = \rho_0^{-1/3}$. In the present study, we scaled all of the lengths in the system by the Gaussian radius of gyration, $R_g \equiv a\sqrt{N/6}$, where a is the monomer statistical Kuhn length. In Eqs. (4) and (7), $\nu_p = -1$ and $\nu_\pm = \pm 1$ are the charge valences of PE chains and mobile ions, respectively. It can be clearly seen from Eqs. (6) and (7) that the electrostatics of SCFT is at the Poisson–Boltzmann level. In Eq. (6) with $M = \pm$, the volume-averaged densities of mobile ions are $\bar{\phi}_+ = \alpha_p\bar{\phi}_p + \bar{\phi}_+^{salt}$ and $\bar{\phi}_- = \bar{\phi}_-^{salt}$. The volume-averaged densities of cations and anions from the added salt are $\bar{\phi}_+^{salt} = \bar{\phi}_-^{salt} = 10^3 a^3 N_A C_s$, where N_A is Avogadro's constant and C_s is the molar concentration of added salt. For $a = 0.7$ nm used in this study, $\bar{\phi}_+^{salt} = \bar{\phi}_-^{salt} \approx 0.207 C_S$. The dimensionless SCF equations for the case of finite-size mobile ions are given in the supplementary material.[41]

The propagators $q_f(\vec{r}, s)$ and $q_g(\vec{r}, s)$ represent the probability of finding the segment s at position $\vec{r}$ with one end free ($q_f(s = 0)$) and the other end grafted on the substrate ($q_g(s = 0)$), respectively. They both satisfy the following modified diffusion equation:

$$\frac{\partial q(\vec{r}, s)}{\partial s} = \nabla^2 q(\vec{r}, s) - \left[\omega_p(\vec{r}) + N\alpha_p\nu_p\psi(\vec{r})\right] q(\vec{r}, s), \tag{8}$$

with the initial conditions $q_g(x, s = 0) = \delta(x - \Delta x)/q_f(x, s = 1)$ and $q_f(x, 0) = 1$, and the boundary conditions $q_f(x = 0, s) = 0$, $q_f(x = D, s) = 0$, $q_g(x = 0, s) = 0$, and $q_g(x = D, s) = 0$.[42,43] Note that the grafting point is shifted from the grafting substrate by one lattice space Δx.

In numerically solving the SCF equations, it is convenient to use the Cartesian coordinate system (x, y, z) in the model setup. Ignoring the edge effect of the electrodes, it is reasonable to assume that all of the physical quantities are independent of the two coordinates, y and z, along the surfaces of the two electrodes, and only vary along the normal direction. Therefore, the problem is reduced from three- (3D) to one-dimensional (1D), and each 3D physical quantity can be viewed as a 1D property on a per unit area in the x direction basis. For the present 1D problem, we adopt the scheme proposed separately by Witte and Meng to compute the monomer volume fraction.[12,37] In this scheme, the initial condition for q_g is $q_g(x = \Delta x, s = 0) = 1$. For the present 1D problem, this scheme of decoupling q_f and q_g in solving the modified diffusion equation should give identical SCF solutions to those obtained from the scheme proposed by Matsen and Muller.[42,43] The only difference between these two schemes is that the incompressibility field $\eta(x)$ will differ by a constant.[40] However, for polymer brushes with two-dimensional (2D) or three-dimensional variation in monomer density, the scheme proposed by Matsen and Muller must be adopted to solve the modified diffusion equation.

The brush height H_B is obtained from the following expression:

$$H_B{}^2 = \frac{\int_0^D x^2\phi_p(x)\,dx}{\int_0^D \phi_p(x)\,dx}. \tag{9}$$

To investigate the distribution of counterions released from the grafted PE chains immersed in a salt-free solution, the fraction of counterions trapped inside the PE brushes δ_+ is introduced as follows:

$$\delta_+ = \frac{\int_0^{H_B} \phi_+(x)\,dx}{\int_0^D \phi_+(x)\,dx}. \tag{10}$$

To verify if charge neutrality is maintained inside the PE brush immersed in a salt-free solution, the degree of charge neutrality Γ_e is defined as follows:

$$\Gamma_e = \frac{\int_0^{H_B}\left[\alpha_p\phi_p(x) + \phi_+(x)\right]dx + \sigma_e}{\int_0^{H_B}\alpha_p\phi_p(x)\,dx}. \tag{11}$$

If $\Gamma_e = 0$, charge neutrality is precisely maintained.

The modified diffusion equation and Poisson equation are solved using the standard multigrid method.[44] The boundary condition for the Poisson equation is $d\psi(x)/dx|_{x=0} = d\psi(x)/dx|_{x=D} = -\sigma_e/\varepsilon$. The obtained electric potential profile is then subtracted from the potential at $x = D$ so that $\psi|_{x=D} = 0$. In the calculation, unless otherwise stated, the grid size of the computational domain is $\Delta x = 0.0625R_g$ and the time step size is $\Delta s = 0.0025$, which corresponds to discretizing the polymer chain spatial thread into 400 equal intervals.

III. RESULTS AND DISCUSSION

The input parameters for the SCFT numerical studies are listed in Table I. The radius of gyration of a neutral Gaussian chain R_g was selected as the length unit to scale all of the relevant physical quantities except for the surface charge and grafting densities. The two parallel electrodes can be neutral or oppositely charged with a surface charge density of σ_e. The product of σ_e and a^2, which is defined as the dimensionless surface charge density, was varied from -1.90×10^{-1} to $+1.90 \times 10^{-1}$, corresponding to charge density of $\sigma_e = -3.89 \times 10^{-1}$ nm^{-2} to $\sigma_e = 3.89 \times 10^{-1}$ nm^{-2}. Such a choice of surface charge densities ensures that the electrostatics of the system remains in the weak coupling regime, in which mean-field SCFT is valid.[42] The dimensionless grafting density $\sigma_g a^2$ was varied from 0.06 to 0.4, which is much lower than the maximum theoretical grafting density of unity. For PE chains grafted on a square lattice, the crossover grafting density σ_g^*, corresponding to the transition from the mushroom to brush regime, can be estimated from the condition $\sigma_g^*(2R_g)^2 = 1$. For parameters used in this study, $\sigma_g^* a^2 = 0.03$. At room temperature, a dimensionless

TABLE I. Input parameters for the SCFT numerical studies.

Monomer size (a)	0.7 nm
Chain length (N)	50
Separation between electrodes (D)	$32R_g$
Flory–Huggins parameter (χ_{PS})	0.0
Dimensionless grafting density (σ_g)	0.06–0.4
Charge fraction (α_p)	0.1–0.4
Dimensionless dielectric permittivity (ε)[a]	4.76×10^{-1}
Dimensionless surface charge density (σ_e)	$(-1.90$ to $1.90)\times10^{-1}$
Molar salt concentration (C_s)	0.0–0.25M
Mobile ion size ($\upsilon_R{}^{1/3}a$)	0 or 0.35 nm

[a] $\varepsilon = 6\varepsilon_0\varepsilon_s a k_B T/(e^2)$, where ε_0 and ε_s are the vacuum permittivity and dielectric constant of the system, respectively. Thus, $\varepsilon = 0.476$ corresponds to the dielectric constant of water at room temperature ($\varepsilon_s = 78$).

electric potential ($\psi_{\text{dimensionless}} = e\psi/k_BT$, where e, k_B, and T are the elementary charge, Boltzmann constant, and absolute temperature, respectively) of 1 corresponds to an electric potential of about 2.52×10^{-2} V. Moreover, a dimensionless electric field strength ($E_{\text{dimensionless}} = EeR_g/k_BT$) of 1 corresponds to an electric field strength of about 1.25×10^7 V/m. In this study, the use of R_g as the length scale to non-dimensionalize and numerically solve the SCFT equations exactly follows Refs. 39 and 40. It should also be pointed out that R_g was also chosen as the length scale in the numerical SCFT studies of the stimuli response of strong polyacid and weak polybase brushes.[37,45] In the dimensionless quantity, the boundary condition for Poisson's equation is $d\psi(x)/dx|_{x=0} = d\psi(x)/dx|_{x=D} = -\sqrt{6N}\sigma_e/\varepsilon$.[44]

A. Response of PE brushes immersed in a salt-free solution to an external electric field

1. Low grafting density regime

From Figures 1 and 2, in the low grafting density regime, a negatively charged electrode grafted with PE chains carrying negative charges leads to an extension of the PE chains and a corresponding increase in the brush height, or vice versa. Taking the brush height at $\sigma_e = 0$ as a reference, the change of the brush height in the parameter range shown in Figure 1 is significant (−23% to 17%). Furthermore, in terms of the magnitude of the gradient of the plot of brush height against surface electric potential (Figure 1), the degree of collapse of PE brushes under a positive surface electric potential or positive voltage is higher than that of the extension of the PE brushes under an applied negative voltage. Evidently, a zero surface charge density does not correspond to a zero surface electric potential or voltage, but rather to a negative surface electric potential. Nevertheless,

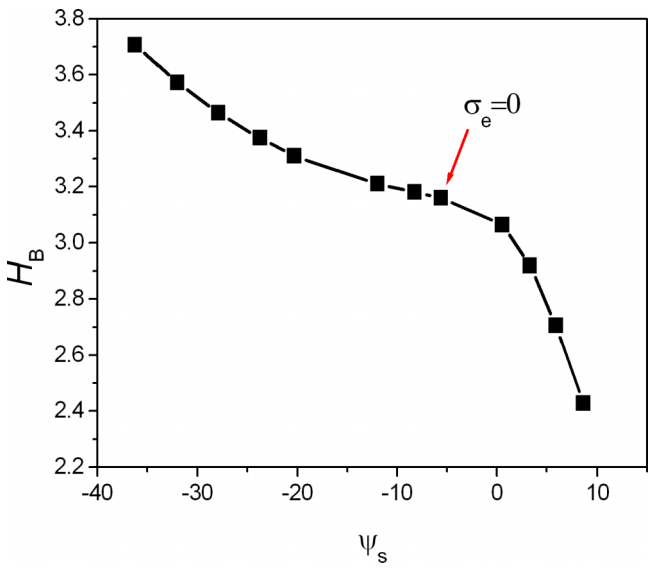

FIG. 1. Brush height plotted against the surface electric potential of the electrode grafted with PE chains. The system parameters are $\alpha_P = 0.1$ and $\sigma_g = 0.06$. The surface charge densities corresponding to the data points from left to right are $\sigma_e = -4.76\times10^{-2}$, -4.17×10^{-2}, -3.57×10^{-2}, -2.98×10^{-2}, -2.38×10^{-2}, -1.19×10^{-2}, -5.95×10^{-3}, 0, 4.76×10^{-2}, 9.52×10^{-2}, 1.43×10^{-1}, and 1.90×10^{-1}. The data point corresponding to $\sigma_e = 0$ is labeled in the figure.

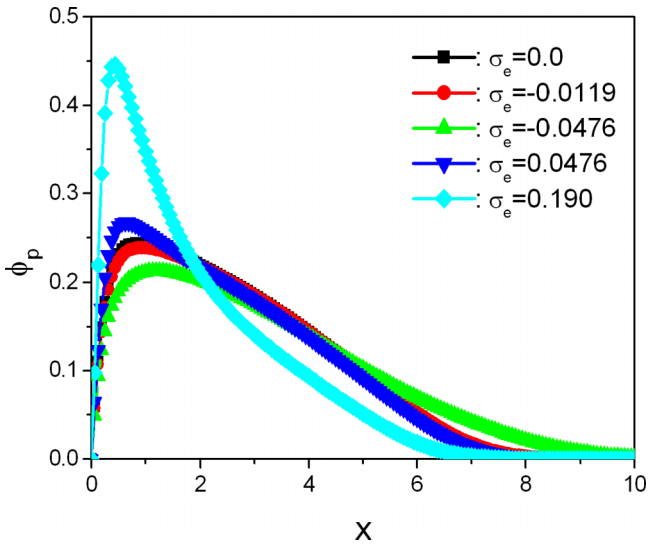

FIG. 2. Monomer density profiles of systems with different surface charge densities (see legend). The other system parameters are $\alpha_P = 0.1$ and $\sigma_g = 0.06$.

there is a one-to-one correspondence between the surface charge density and surface electric potential. It should be pointed out that in the model setup and numerical solution of the SCF equations, a voltage across the two parallel electrodes could be applied directly. After obtaining the electric potential profile by solving Poisson equation with Dirichlet boundary condition for the electric potential, the electric field on the surface of the electrode grafted with PE chains can be calculated, which gives the surface charge density ($E = \sigma_e/\varepsilon$). In terms of the one-to-one correspondence between the surface charge density and the surface electric potential, this scheme should be equivalent to that used in this study, where equal but opposite surface charges were applied on the two electrodes and the surface potential was extracted after solving the Poisson equation. It should be pointed out that numerical instability prevents more negative surface charge density than -4.76×10^{-2} from being investigated. Our algorithm converged nicely in the whole range of positive surface charge densities used in this study. However, the convergence was rather poor for PE chains grafted onto a negatively charged electrode and immersed in a salt-free solution. The poorer convergence in the latter case can be attributed to the negative monomer charges at the grafting point being only one lattice spacing Δx from the grafting electrode with negative surface charges, which is very energetically unfavorable compared with the former case where the grafting electrode is covered with positive surface charges. The electrostatic coupling parameter Ξ ($\Xi = l_B/\mu = 2\pi l_B{}^2\sigma_e$ with l_B and μ are the Bjerrum length and the Gouy-Chapman length, respectively) proposed by Netz *et al.*[46] at the highest surface charge density ($\sigma_e = 3.89 \times 10^{-1}$ nm^{-2}) applied in this study is about 1.2, which suggests that the electrostatics in this study is very close to the weakly coupling regime. Therefore, in the parameter range of the surface charge density applied in this study, it is very unlikely that the assumption of one-dimensional variations of all of the physical quantities will break down.

Nonetheless, for the most negative surface charge densities on the grafting electrode investigated in this study, the

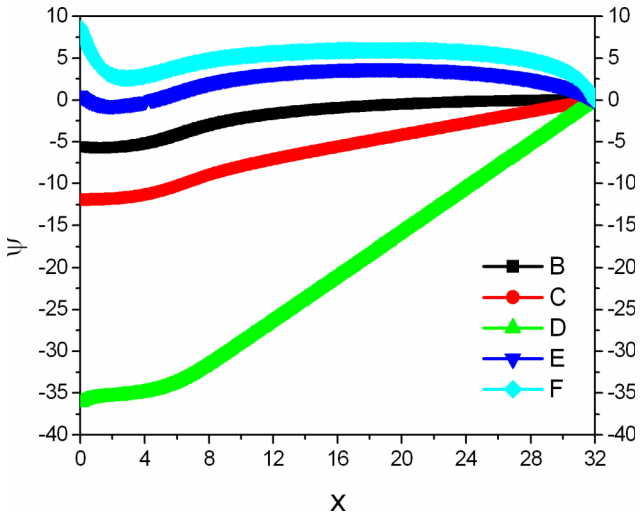

FIG. 3. Electric potential profiles of systems with different surface charge densities. The surface charge densities corresponding to legends **B** to **F** are, respectively, 0, -1.19×10^{-2}, -4.76×10^{-2}, 4.76×10^{-2}, and 1.90×10^{-1}. For reference, the electric potential profiles in the absence of grafted PE brushes are included in the supplementary material.[41] It should be pointed out that, for the present strong PE brushes with the smeared charge distribution, a uniform shift in the electric potential such that the electric potential on the second electrode is zero has no influence on the SCF solutions.[40]

voltage was in the range of −36 to −10 (corresponding to −0.9 to −0.25 V), which is in the experimentally relevant parameter regime of applied voltage.[32]

As expected, the electric potential profile across the two parallel electrodes shifts toward a higher electric potential when increasing surface charge density from negative to positive on the electrode grafted with PE chains (see Figure 3). However, the electric field profile across the two electrodes is highly non-trivial, as shown in Figure 4. A salient feature of the electric field profile in the region from 2 to 3 times the brush height from the grafting substrate (~$8R_g$, see the inset of Figures 4 and 2) is the non-uniformity of the electric field.

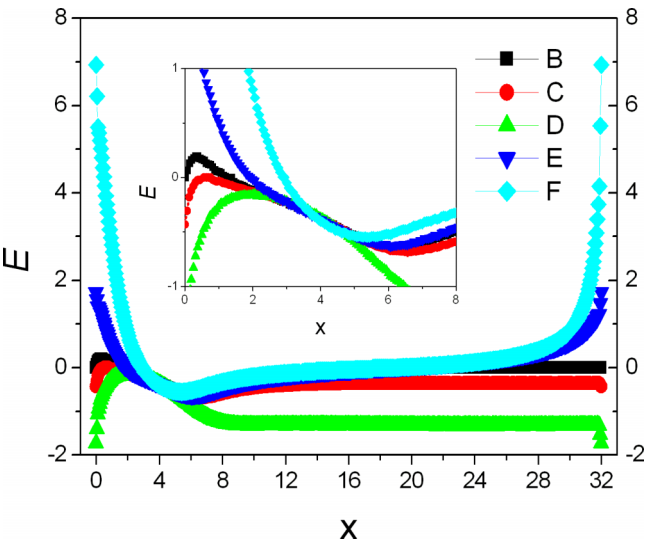

FIG. 4. Electric field profiles of systems with different surface charge densities. The surface charge densities corresponding to legends **B** to **F** are, respectively, 0, -1.19×10^{-2}, -4.76×10^{-2}, 4.76×10^{-2}, and 1.90×10^{-1}. The inset shows an enlargement of the electric field profile near the grafting substrate.

From the perspective of MD simulation, as well as the other forces acting on each monomer, each monomer will experience an electric force $\vec{F} = -\alpha_p |e| \vec{E}$ because of the applied surface charges or voltage. However, the highly non-uniform electric field across the two parallel electrodes is generated by all of the charges in the system, i.e., surface charges on the electrodes, monomer charges, and counterions. For surface charge density below $\sigma_e = -1.19 \times 10^{-2}$ (see inset in Figure 4), the electric field will exert an electric force on all of the monomers directed towards the positive x direction, which tends to stretch the PE chains. Conversely, for the case of $\sigma_e = 1.90 \times 10^{-1}$, the monomers inside the brush region defined by the brush height (~$2.4R_g$), which is the majority of the monomers, will experience non-uniform electric forces pointing in the negative x direction. Electric forces in the positive x direction will be exerted on the monomers extending further away from the grafting substrate. In essence, the external electric field generated by the opposite surface charges on the two electrodes, which would otherwise be uniform between the two electrodes, is strongly modified by the PE brush grafted on one electrode.

2. *Intermediate and high grafting density regimes*

As shown in Figure 5, the gradient of the plot of brush height against voltage at $\sigma_g = 0.1$ is much higher than that at $\sigma_g = 0.2$. From Figure 5, the relative changes in the brush height with respect to the reference height at $\sigma_e = 0$ are comparable for the two cases with the same grafting density of $\sigma_g = 0.1$. In the range of the applied voltage (−18 to 4) for the case of $\alpha_p = 0.2$ and $\sigma_g = 0.1$ shown in Figure 5, the relative changes in the brush height with respect to the reference height at $\sigma_e = 0$ are about −6.5% to 5.0%. However, for $\sigma_g = 0.2$, the relative changes are only about −1.8% to 1.4% in the same voltage range. At an even higher grafting density, e.g., $\sigma_g = 0.4$, the brush height becomes quite insensitive to the applied

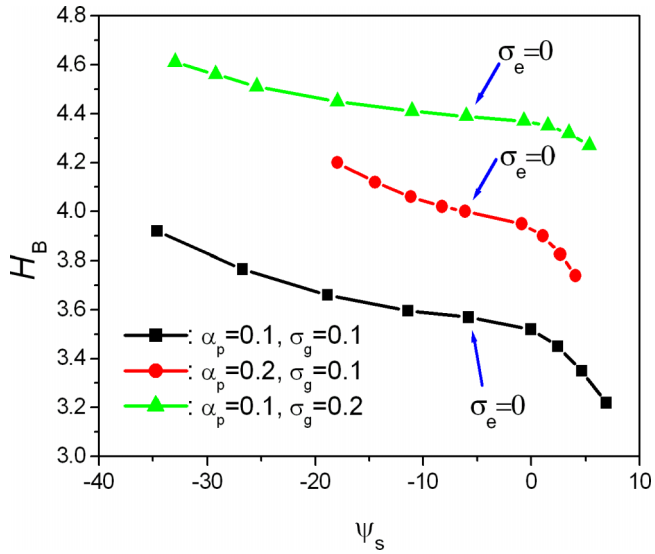

FIG. 5. Plots of brush height against surface electric potential of the electrode grafted with PE chains for different grafting densities and charge fractions. The system parameters are shown in the legend. The surface charge densities corresponding to the different data points in the figure are listed in the supplementary material.[41] The data points corresponding to $\sigma_e = 0$ are labeled in the figure.

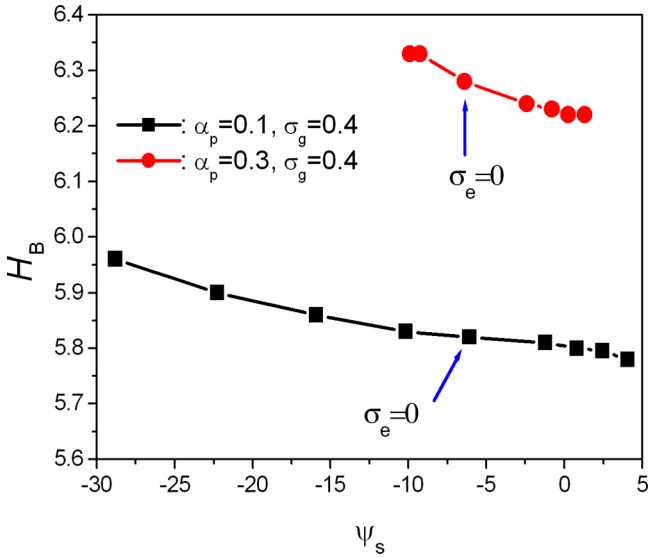

FIG. 6. Plots of the brush height against surface electric potential of the electrode grafted with PE chains for two different charge fractions of PE chains and the same grafting density of $\sigma_g = 0.4$ (see legend). The surface charge densities corresponding to the different data points in the figure are listed in the supplementary material.[41] The data points corresponding to $\sigma_e = 0$ are labeled in the figure. It should be pointed out that numerical stability prevents investigation of the case with $\sigma_g = 0.4$ and $\alpha_P = 0.3$ for applied surface charge densities more negative than -1.79×10^{-2}.

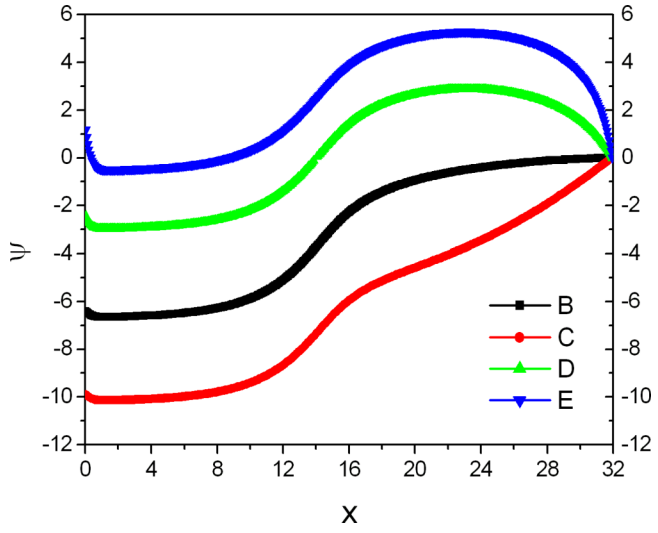

FIG. 8. Electric potential profiles of systems with different surface charge densities. The legends in terms of surface charge densities are the same as those in Figure 7.

voltage (see Figure 6). For the case of $\sigma_g = 0.4$ and $\alpha_p = 0.1$, in the whole range of applied voltage, the relative change in brush height is only about ±1.5%. Moreover, the monomer density profile at $\sigma_g = 0.4$ is barely perturbed by the applied surface charge or voltage, as shown in Figure 7. Therefore, the grafting density plays a much more important role than the charge fraction in controlling the response of PE brushes to an external electric field. For $\sigma_g > 0.2$, the brush height becomes nearly independent of the applied voltage across the two electrodes. In the MD simulations of the extension of PE brushes subject to normal electric fields, the brush height remains constant in weak electric fields.[38] The critical electric field strength is defined such that the relative increase in the brush height is >5% above this value. The critical electric field strength was found to increase with increasing grafting density of the PE brushes. The finding in this study that a higher grafting density of the PE brushes requires a larger magnitude of applied voltage across the two electrodes to achieve the same amount of relative change in the brush height is consistent with the MD simulation result, although direct and quantitative comparison is difficult.

A typical example of the electric potential profiles across the two parallel electrodes at high grafting density is shown in Figure 8. Figure 9 and its inset show that the electric field profiles for different surface charge densities at high grafting density overlap from the region near the grafting electrode to the middle of the system, which is in sharp contrast to the case

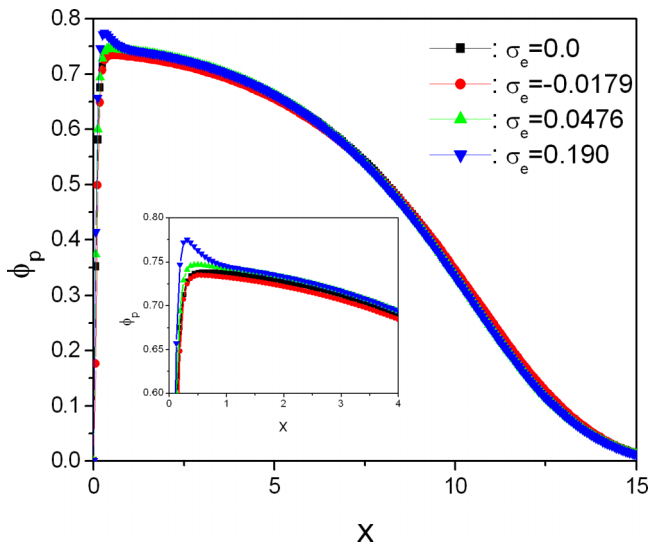

FIG. 7. Monomer density profiles of the systems for different surface charge densities (see the legend). The other system parameters are $\alpha_P = 0.3$ and $\sigma_g = 0.4$. The inset shows an enlargement of the profiles near the grafting substrate.

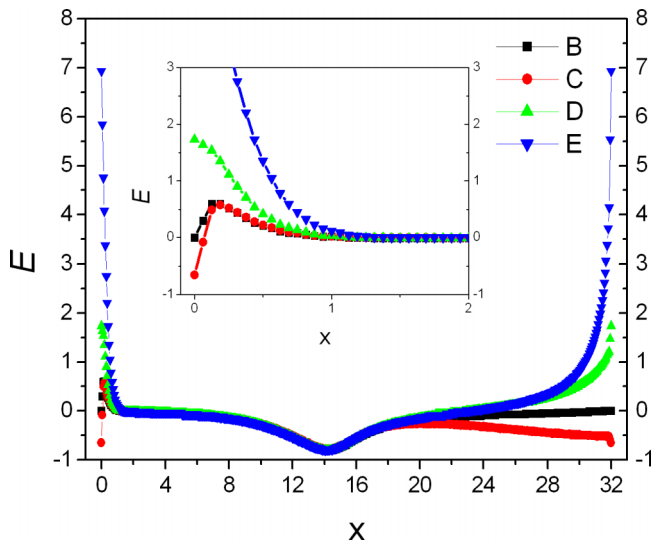

FIG. 9. Electric field profiles of systems with different surface charge densities. The legends in terms of surface charge densities are the same as those in Figure 7. The inset shows enlargements of the electric field profiles near the grafting electrode.

of low grafting density shown in Figure 4. Furthermore, the electric field is nearly zero in the region between the positions with coordinates $1R_g$ and $6R_g$, which means that a significant number of monomers would not experience any electric forces in the molecular simulations. In addition, as shown in the inset of Figure 9, the applied surface charges on the electrodes only modify the electric field in the region very close to the grafting electrode, which is drastically different to the case of low grafting density shown in Figure 4. The much stronger resistance of the local electric field of PE brushes to perturbation by applied surface charge or voltage at high grafting density compared with at low grafting density is the reason for the insensitivity of the response of PE brushes with high grafting density to an externally applied voltage observed in this study.

3. Amount of trapped counterions and overall charge balance inside PE brushes

The effect of the applying opposite surface charges to the two electrodes on the fraction of counterions trapped inside the PE brushes was investigated, and the results are shown in Figure 10. In the absence of surface charges on the electrodes, the fraction of trapped counterions inside the PE brushes δ_+ was about 0.62, irrespective of the grafting density and the charge fraction of the PE chains. Figure 10 clearly shows that δ_+ is a decreasing function of surface charge density on the grafting electrode. This is because the positively charged counterions would be more strongly repelled by the more positively charged electrode grafted with PE chains. Furthermore, the magnitude of the slope of the curve decreases with increasing grafting density and charge fraction of the PE chains because PE brushes with higher grafting density and charge fraction can retain the counterions more strongly through electrostatic attractions. For PE brushes with $\sigma_g = 0.4$ and $\alpha_p = 0.3$, δ_+ barely changes in the parameter range of surface charge density. Therefore, in the high grafting density regime, PE brushes become quite insensitive to the applied voltage.

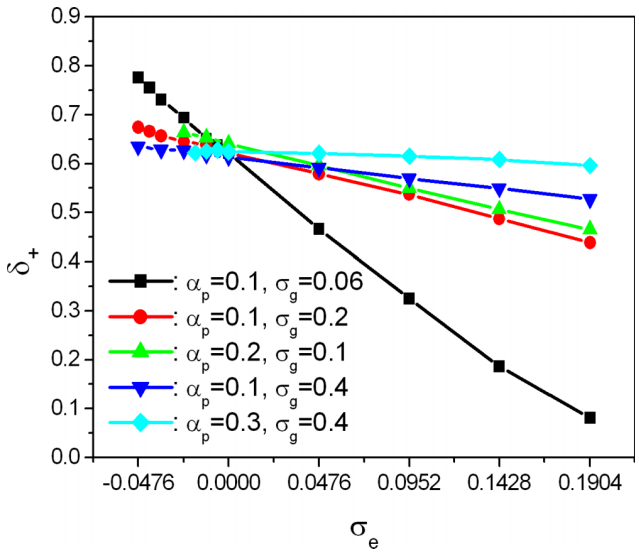

FIG. 10. Fraction of counterions trapped inside the PE brush as a function of the surface charge density for systems with different charge fractions and grafting densities (see the legend for parameters). The PE brush is immersed in a salt-free solution.

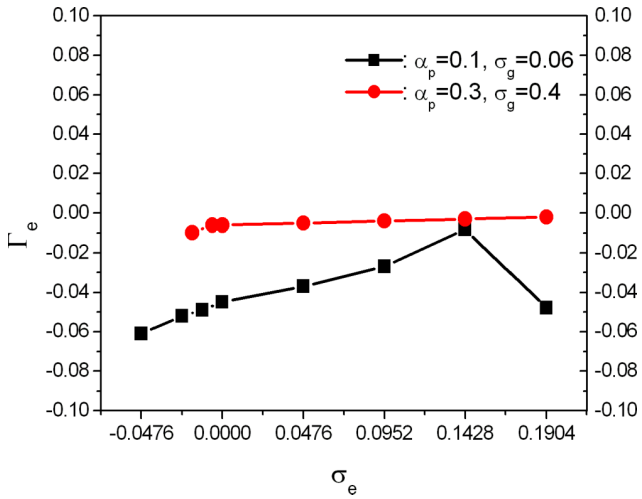

FIG. 11. Plots of the degree of charge compensation inside the PE brush as a function of the surface charge density for systems with different charge fractions and grafting densities (see the legend for the system parameters).

The overall charge neutrality inside the PE brush in the presence of surface charges on the electrodes is quantified by the degree of charge compensation Γ_e, which includes the contribution of surface charges. The results are shown in Figure 11 and indicate that the deviation from overall charge neutrality inside the PE brush is small, especially for PE brushes with high grafting density and charge fraction. Thus, the applied surface charges on the electrodes have a very weak influence on the overall charge balance inside the PE brush.

B. Effect of added salt on the response of PE brushes to an external electric field

The influence of added salt ions on the brush height of PE brushes in the absence of applied surface charges on the electrodes was first investigated, and the results are shown in Figure 12. At zero salt concentration, the Debye screening

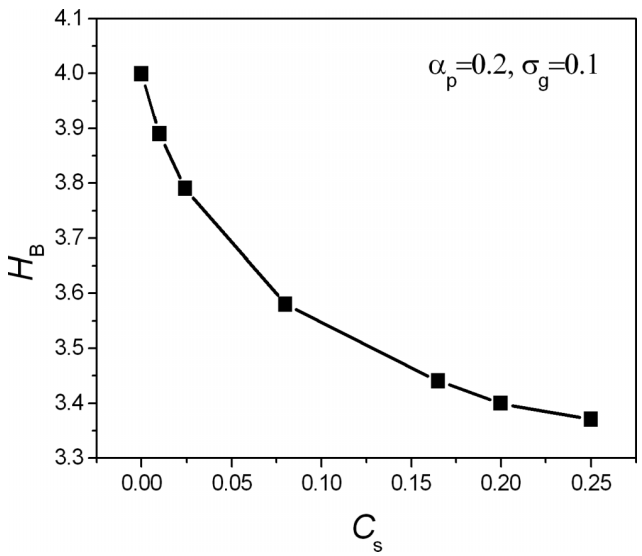

FIG. 12. Brush height plotted against molar concentration of added salt in the absence of applied surface charges on the electrodes. The system parameters are shown in the figure.

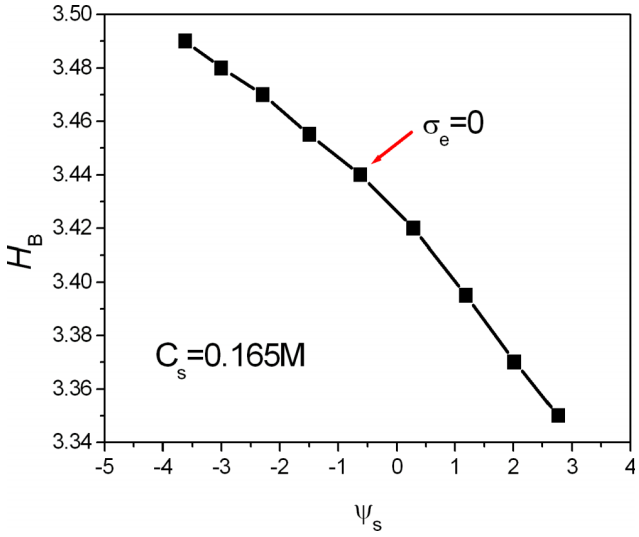

FIG. 13. Brush height plotted against the surface electric potential of the electrode grafted with PE chains with $\alpha_P = 0.2$ and $\sigma_g = 0.1$ at a salt concentration of 1.65×10^{-1}M. The surface charge densities corresponding to the data points from left to right are $\sigma_e = -1.90\times10^{-1}$, -1.43×10^{-1}, -9.52×10^{-2}, -4.76×10^{-2}, 0, 4.76×10^{-2}, 9.52×10^{-2}, 1.43×10^{-1}, and 1.90×10^{-1}. The data point corresponding to $\sigma_e = 0.0$ is labeled in the figure.

length is about 1.90 nm. At $C_s = 1.65\times10^{-1}$M, the Debye screening length is about 0.70 nm, which is the same as the monomer size a. By comparing the red curve in Figure 5 with Figure 13, it can be clearly seen that the relative change in brush height with respect to $\sigma_e = 0$ is greatly reduced with the addition of a relatively high concentration of salt. Therefore, the response of PE brushes to the external electric field becomes much weaker in the high-salt regime compared with the salt-free case. In addition, the span of surface electric potential or the applied voltage is reduced in the high salt regime because of much stronger electrostatic screening from salt ions. An interesting feature of Figure 13 is that the brush height almost linearly decreases with increasing applied positive voltage. In a theoretical study of the collapse of PE brushes sandwiched between two parallel electrodes in response to an externally applied voltage, Yamamoto and Pincus predicted that the brush height almost linearly decreases with increasing voltage in the high-salt regime.[36] This theoretical prediction is strongly supported by our present numerical results. Moreover, in the low-salt regime, they predicted that the brush height rapidly decreases with increasing voltage between the two electrodes. The rapid decrease of brush height in response to an applied positive voltage in a salt-free solution in Figures 2 and 5 is consistent with the prediction of Yamamoto and Pincus.

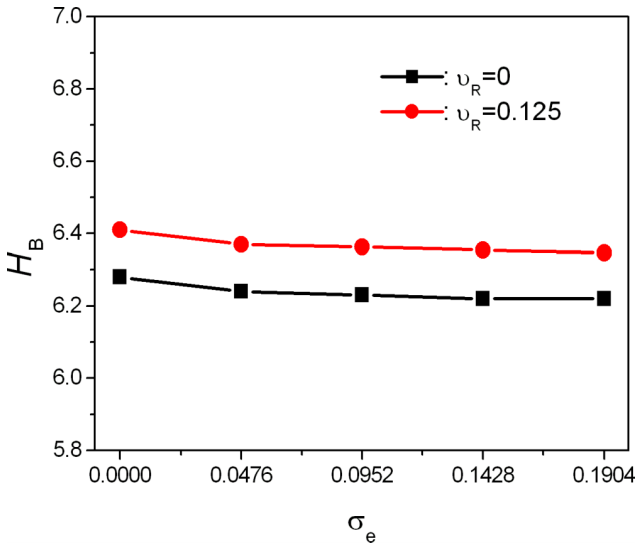

FIG. 14. Brush height plotted as a function of surface charge density for the cases of point charges and finite-size mobile ions. The system parameters are $\alpha_P = 0.3$ and $\alpha_g = 0.4$. The PE brush is immersed in a salt-free solution.

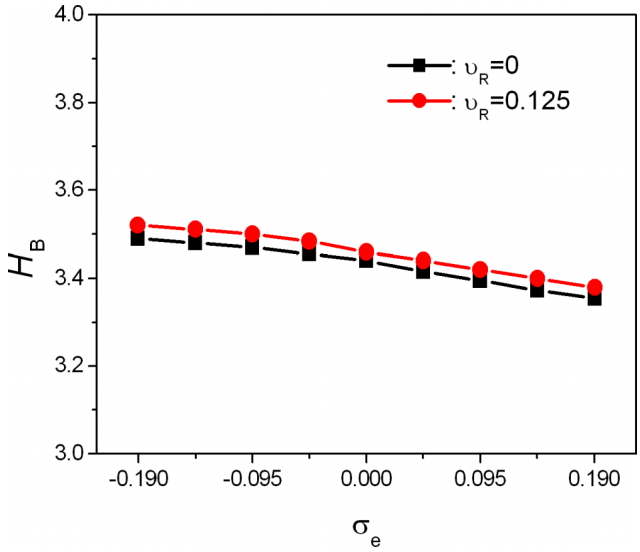

FIG. 15. Brush height plotted as a function of the surface charge density for the cases of point charges and finite-size mobile ions. The system parameters are $\alpha_P = 0.2$, $\sigma_g = 0.1$, and $C_s = 0.165$M.

C. Effect of mobile ion size on the response of PE brushes to an external electric field

In Secs. III A and III B, mobile ions were assumed to be point charges. The influence of mobile ion size on the variation of the brush height with an external electric field was also investigated, and the results are shown in Figures 14 and 15. When mobile ions are half the size of the monomer, the brush height only differs by about 2% compared with the point charge case, as shown in Figure 14. Figure 15 shows that the difference in the brush height is even smaller in the high-salt regime. When the mobile ion size increases, the difference in the brush height becomes more significant (data not shown). Therefore, the effect of mobile ion size on the brush height is quite weak if the mobile ions are no more than half the size of the monomer. Moreover, it is worth pointing out that the size of small ions would play an insignificant role in the behavior of PE brushes if the grafting density is not very high, where the excluded volume effect is weak.[45]

IV. CONCLUSIONS

In this paper, the response of strong PE brushes grafted on an electrode to applied electric fields across the electrode and a second parallel electrode was numerically investigated by SCFT. The electric fields were generated by opposite surface charges on the two electrodes. There was a one-to-one

correspondence between the surface charge density and the voltage across the two electrodes. Such a model setup makes direct and quantitative comparison with corresponding experiments possible. The influences of grafting density, average charge fraction, salt concentration, and mobile ion size on the variation of the brush height with the applied voltage bias were investigated. The distribution of counterions and overall charge neutrality inside the PE brush were also investigated.

The numerical results clearly show that there is considerable extension and contraction of the PE brush in response to applied voltages when the grafting density is low. Consistent with MD simulation results, a higher grafting density requires a larger voltage to achieve the same relative change in the brush height. In the experimentally relevant parameter regime of the applied voltage, the brush height becomes insensitive to the voltage bias for sufficiently high grafting density. The numerical results further reveal that the electric field inside the PE brush is highly non-uniform, because of the complex interplay between the surface charges, charges on grafted PE chains, and counterions. When including the contribution of surface charges on the grafting electrode, overall charge neutrality is generally maintained inside PE brushes, especially for PE brushes with high grafting density and average charge fraction.

The brush height of negatively charged PE chains was found to rapidly decrease in response to applied positive voltage in a salt-free solution. Our numerical study also showed that the brush height almost linearly decreases with increasing positive voltage across the two electrodes for PE brushes in the high-salt regime. Such different trends agree with the theoretical predictions of Yamamoto and Pincus.[36] Furthermore, as far as the brush height is concerned, the results demonstrate that the point charge assumption for mobile ions is reasonable when the mobile ions are small compared with the monomer and the grafting density is not very high.

It should be noted that SCFT used in this study is a mean-field theory and is only applicable to weakly charged polymeric systems. Thus, it is unlikely that the PE brush surface undulation proposed by Tsori[35] and the splitting of PE brushes into two subpopulations observed in MD simulations[38] can be captured by 2D or 3D numerical SCFT studies. Furthermore, dielectric mismatch among the non-polar polymer chain backbone, metallic electrode, and polar solvent is not considered in this study.[47–49] These issues could be the focus of future studies about the response of PE brushes to external electric fields. Finally, it is worth pointing out that the numerical SCFT study of the response of weak PE brushes to external electric fields demonstrates that the brush height is independent of the applied electric field at intermediate and high grafting densities,[45] which is consistent with experimental observations.[50] We hope that the present study will stimulate experimental research interest of the response of strong PE brushes to external electric fields.

ACKNOWLEDGMENTS

The authors thank the financial supports from the National Natural Science Foundation of China (NSFC Project No. 21374052). C.T. acknowledges the support from K. C. Wong Magna Fund in Ningbo University.

[1]J. Rühe, M. Ballauff, M. Biesalski, P. Dziezok, F. Grohn, D. Johannsmann, N. Houbenov, N. Hugenberg, R. Konradi, S. Minko, M. Motornov, R. R. Netz, M. Schmidt, C. Seidel, M. Stamm, T. Stephan, D. Usov, and H. N. Zhang, Adv. Polym. Sci. **165**, 79 (2004).
[2]A. Halperin, M. Tirrell, and T. P. Lodge, Adv. Polym. Sci. **100**, 31 (1992).
[3]A. Naji, C. Seidel, and R. R. Netz, Adv. Polym. Sci. **198**, 149 (2006).
[4]D. H. Napper, in *Polymeric Stabilization of Colloidal Dispersions* (Academic Press, London, 1983), Vol. 7.
[5]P. Pincus, Macromolecules **24**, 2912 (1991).
[6]O. V. Borisov, T. M. Birshtein, and E. B. Zhulina, J. Phys. II **1**, 521 (1991).
[7]O. V. Borisov, E. B. Zhulina, and T. M. Birshtein, Maromolecules **27**, 4795 (1994).
[8]R. Israëls, F. A. M. Leermakers, G. J. Fleer, and E. B. Zhulina, Macromolecules **27**, 3249 (1994).
[9]E. B. Zhulina and O. V. Borisov, J. Chem. Phys. **107**, 5952 (1997).
[10]R. R. Netz and D. Andelman, Phys. Rep. **380**, 1 (2003).
[11]A. Naji, R. R. Netz, and C. Seidel, Eur. Phys. J. E **12**, 223 (2003).
[12]K. N. Witte, S. Kim, and Y. Y. Won, J. Phys. Chem. B **113**, 11076 (2009).
[13]F. S. Csajka, R. R. Netz, C. Seidel, and J.-F. Joanny, Eur. Phys. J. E **4**, 505 (2001).
[14]C. Seidel, Macromolecules **36**, 2536 (2003).
[15]O. J. Hehmeyer and M. J. Stevens, J. Chem. Phys. **122**, 134909 (2005).
[16]O. J. Hehmeyer, G. Arya, A. Z. Panagiotopoulos, and I. Szleifer, J. Chem. Phys. **126**, 244902 (2007).
[17]N. A. Kumar and C. Seidel, Phys. Rev. E **76**, 02080 (2007).
[18]A. Wynveen and C. N. Likos, Phys. Rev. E **80**, 010801 (2009).
[19]P. Linse, J. Chem. Phys. **126**, 114903 (2007).
[20]D. Russano, J.-M. Y. Carrillo, and A. V. Dobrynin, Langmuir **27**, 11044 (2011).
[21]L. Sjöström, T. Akesson, and B. J. Jönsson, J. Chem. Phys. **99**, 4739 (1993).
[22]Y. P. Ou, J. B. Sokoloff, and M. J. Stevens, Phys. Rev. E **85**, 011801 (2012).
[23]S.-Z. He, H. Merlitz, L. Chen, J.-U. Sommer, and C.-X. Wu, Macromolecules **43**, 7845 (2010).
[24]P. Malfreyt and D. J. Tildesley, Langmuir **16**, 4732 (2000).
[25]M. Sirchabesan and S. Giasson, Langmuir **23**, 9713 (2007).
[26]C. Ibergay, P. Malfreyt, and D. J. Tildesley, J. Phys. Chem. B **114**, 7274 (2010).
[27]J. Yang and D. P. Cao, J. Phys. Chem. B **113**, 11625 (2009).
[28]H. Ouyang, Z. H. Xia, and J. Zhe, Nanotechnology **20**, 195703 (2009).
[29]Q. Q. Cao, C. C. Zuo, L. J. Li, and G. Yan, Biomicrofluidics **5**, 044119 (2011).
[30]Q. Q. Cao, C. C. Zuo, L. J. Li, Y. H. Zhang, and G. Yan, J. Polym. Sci., Part B: Polym. Phys. **50**, 805 (2012).
[31]H. Ouyang, Z. H. Xia, and J. Zhe, Microfluid. Nanofluid. **9**, 915 (2010).
[32]F. Zhou, P. M. Biesheuvel, E.-Y. Choi, W. Shu, R. Poetes, U. Steiner, and W. T. S. Huck, Nano Lett. **8**, 725 (2008).
[33]G. J. Dunderdale and J. P. A. Fairclough, Langmuir **29**, 3628 (2013).
[34]G. Migliorini, Macromolecules **43**, 9168 (2010).
[35]Y. Tsori, D. Andelman, and J. F. Joanny, Europhys. Lett. **82**, 46001 (2008).
[36]T. Yamamoto and P. A. Pincus, Europhys. Lett. **95**, 48003 (2011).
[37]D. Meng and Q. Wang, J. Chem. Phys. **135**, 224904 (2011).
[38]Y. F. Ho, T. N. Shendruk, G. W. Slater, and P. Y. Hsiao, Langmuir **29**, 2359 (2013).
[39]A. C. Shi and J. Noolandi, Macromol. Theory Simul. **8**, 214–229 (1999).
[40]Q. Wang, T. Taniguchi, and G. H. Fredrickson, J. Phys. Chem. B **108**, 6733–6744 (2004).
[41]See supplementary material at http://dx.doi.org/10.1063/1.4927814 for the SCF equations in the case of finite-size mobile ions, electric potential profile across the two oppositely charged electrodes in the absence of PE brushes with pure water or electrolyte aqueous solutions confined between the two electrodes, and the dimensionless quantities of surface charge densities corresponding to the different data points in the plots shown in Figures 5 and 6.
[42]J. U. Kim and M. W. Matsen, Macromolecules **41**, 246 (2008).
[43]M. Muller, Phys. Rev. E **65**, 030802 (2002).
[44]C. Tong, Y. Zhu, H. D. Zhang, F. Qiu, P. Tang, and Y. L. Yang, J. Phys. Chem. B **115**, 11307 (2011).
[45]C. Tong, Langmuir **30**, 15301 (2014).
[46]A. Naji, S. Jungblut, A. G. Moreira, and R. R. Netz, Physica A **352**, 131 (2005).
[47]I. Nakamura, A. C. Shi, and Z. G. Wang, Phys. Rev. Lett. **109**, 257802 (2012).
[48]R. Wang and Z. G. Wang, Phys. Rev. Lett. **112**, 136101 (2014).
[49]R. Kumar, B. G. Sumpter, and S. M. Kilbey II, J. Chem. Phys. **136**, 234901 (2012).
[50]M. P. Weir, S. Y. Heriot, S. J. Martin, A. J. Parnell, S. A. Holt, J. R. P. Webster, and R. A. L. Jones, Langmuir **27**, 11000 (2011).